Inorganic Chemistry

Article

pubs.acs.org/IC

Monopicolinate Cross-Bridged Cyclam Combining Very Fast Complexation with Very High Stability and Inertness of Its Copper(II) Complex

Luís M. P. Lima,[‡] Zakaria Halime,[†] Ronan Marion,[†] Nathalie Camus,[†] Rita Delgado,*[,‡] Carlos Platas-Iglesias,[§] and Raphaël Tripier*[,†]

[‡]Instituto de Tecnologia Química e Biológica, Universidade Nova de Lisboa, Av. da República, 2780-157 Oeiras, Portugal

[†]Université de Bretagne Occidentale, UMR-CNRS 6521, UFR des Sciences et Techniques, 6 avenue Victor le Gorgeu, C.S. 93837, 29238 Brest Cedex 3, France

[§]Departamento de Química Fundamental, Universidade da Coruña, Campus da Zapateira, Rúa da Fraga 10, 15008 A Coruña, Spain

Supporting Information

ABSTRACT: The synthesis of a new cross-bridged 1,4,8,11-tetraazacyclotetradecane (cb-cyclam) derivative bearing a picolinate arm (H**cb-te1pa**) was achieved by taking advantage of the proton sponge properties of the starting constrained macrocycle. The structure of the reinforced ligand as well as its acid−base properties and coordination properties with Cu^{2+} and Zn^{2+} was investigated. The X-ray structure of the free ligand showed a completely preorganized conformation that lead to very fast copper(II) complexation under mild conditions (instantaneous at pH 7.4) or even in acidic pH (3 min at pH 5) at room temperature and that demonstrated high thermodynamic stability, which was measured by potentiometry (at 25 °C and 0.10 M in KNO_3). The results also revealed that the complex exists as a monopositive copper(II) species in the intermediate pH range. A comparative study highlighted the important selectivity for Cu^{2+} over Zn^{2+}. The copper(II) complex was synthesized and investigated in solution using different spectroscopic techniques and DFT calculations. The kinetic inertness of the copper(II) complex in acidic medium was evaluated by spectrophotometry, revealing the very slow dissociation of the complex. The half-life of 96 days, in 5 M $HClO_4$, and 465 min, in 5 M HCl at 25 °C, show the high kinetic stability of the copper(II) chelate compared to that of the corresponding complexes of other macrocyclic ligands. Additionally, cyclic voltammetry experiments underlined the perfect electrochemical inertness of the complex as well as the quasi-reversible Cu^{2+}/Cu^{+} redox system. The coordination geometry of the copper center in the complex was established in aqueous solution from UV−vis and EPR spectroscopies.

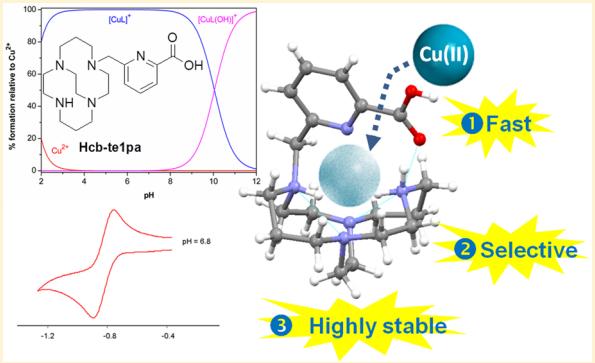

INTRODUCTION

Among the range of potentially useful metals in nuclear medicine, copper has received much interest because it can exist as several radionuclides with different half-lifes and emission properties that are suitable for diagnostic imaging or therapeutic applications and because of the recent increase in the availability of most of these nuclides.[1,2] The most interesting nuclides are the minimally available ^{67}Cu ($t_{1/2}$ = 62.0 h, β^- 100%, E_{max} = 0.577 MeV), which is used for radiotherapy, and, mainly, the now widely available ^{64}Cu ($t_{1/2}$ = 12.7 h, β^+ 17.4%, E_{max} = 0.656 MeV, β^- 39.6%, E_{max} = 0.573 MeV), which is used both for positron emission tomography (PET) and radiotherapy.[1−3]

Copper exists predominantly as a divalent metal cation that exhibits a borderline softness character that prefers donor atoms such as amines and anionic carboxylates to form complexes with coordination numbers of 4−6. High coordination numbers are usually preferred, which often provide square pyramidal, trigonal bipyramidal, or octahedral geometries, so that the metal cation is entirely surrounded.[1,2,4,5] Within the vast range of acyclic and cyclic ligands that have been successfully used for copper(II) complexation, the family of tetraaza macrocycles with N-appended coordinating arms stands out for the efficiency and versatility of their copper chelation.[1,2,4,6] To improve the efficiency of radiopharmaceuticals, it is useful to append a targeting biomolecule on the chelating moiety to induce site-specific delivery of the radiation, producing a bifunctional chelator (BFC).[6−9] Obtaining a BFC requires introduction of an appropriate conjugation group in the structure of the metal chelator, which allows for bioconjugation prior to or after labeling with the radioisotope.

Chelators suitable for copper(II) radiopharmaceuticals are generally those that yield thermodynamically stable and

Received: March 2, 2014
Published: April 23, 2014

   dx.doi.org/10.1021/ic500491c | Inorg. Chem. 2014, 53, 5269−5279

Chart 1. Structure of the Ligands Discussed in This Work

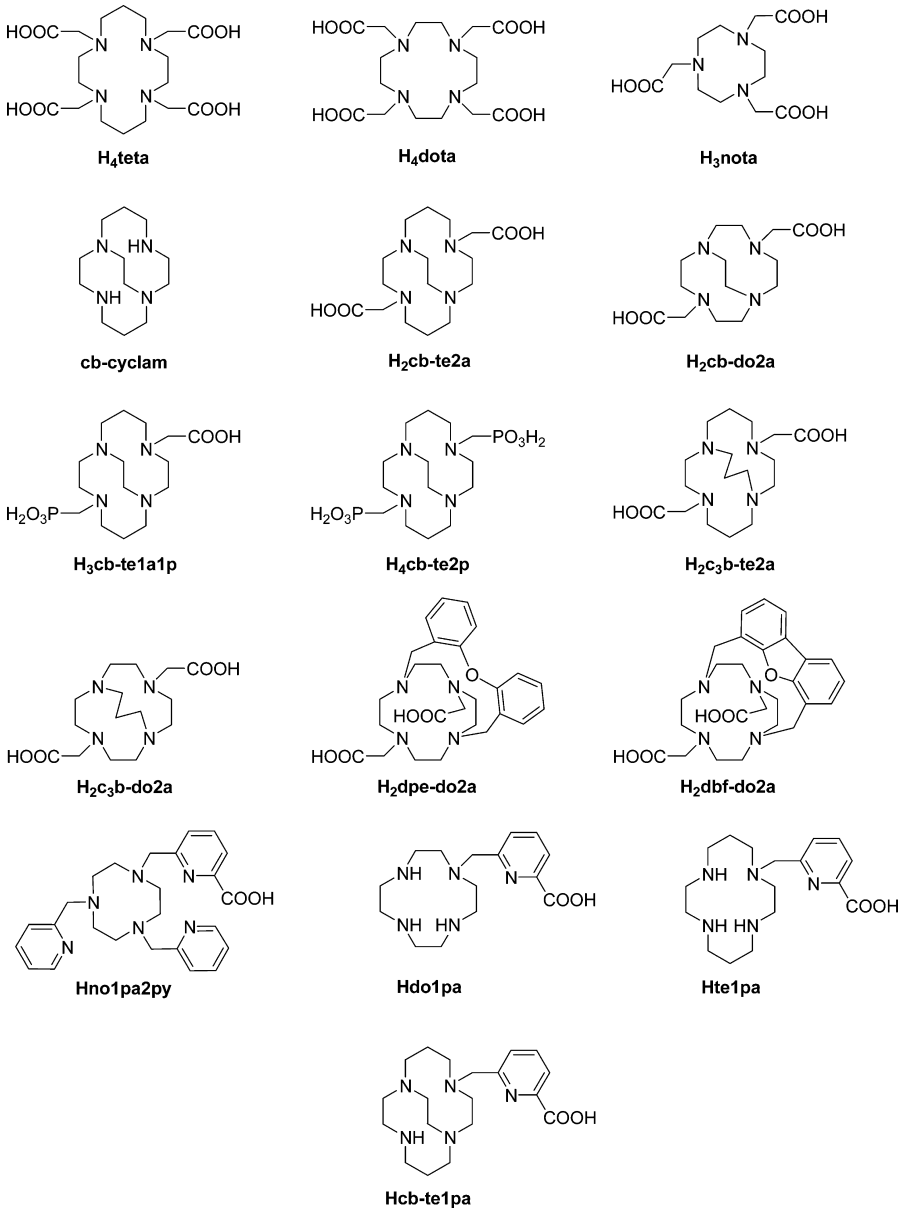

kinetically inert complexes so that possible transchelation of the metal by competing with biological ligands or bioreductants is avoided, whereas other preferred properties include good water solubility and fast metal complexation.[1,2,4,6,7] A special type of rigid tetraaza macrocycles, named cross-bridged chelators, has been a source of great interest because of the outstanding behavior of their copper(II) complexes.[1,2,4−6] These chelators contain an ethylene linker (or, in some cases, a special bridging function as a dibenzofuran, a diphenylether, or a pyridyl group) connecting two trans nitrogen atoms of the macrocycle (Chart 1 shows representative examples), and they have originated some of the most inert copper(II) complexes ever reported.[10−12] Furthermore, successful radiolabeling and bioconjugation of a few examples have also been achieved.[13−17]

One of the biggest challenges of finding ligands that are potentially useful for copper(II) radiopharmaceuticals is the need to combine high thermodynamic stability and kinetic inertness of the complexes with fast metal complexation under mild conditions. Fast complexation is crucial to take full advantage of the short radioisotope half-life times and to allow the use of heat- and pH-sentitive biomolecules. Starting from the established properties of ethylene cross-bridged tetraaza macrocycles, methylenephosphonate pendant arms have been introduced to the macrocycle for that purpose and were found to effectively accelerate complexation rates on cross-bridged cyclam derivatives.[18,19] Picolinate arms have been demonstrated to induce a strong coordination ability toward transition and post-transition metals when appended on macrocyclic[20] and nonmacrocyclic ligands.[21−23] Previously, we developed monopicolinate derivatives of cyclen and cyclam, Hdo1pa and Hte1pa, and studied their copper(II) complexation properties; we found that they readily form thermodynamically stable and kinetically inert complexes, particularly with the later ligand (Chart 1).[24,25] We also developed a triaza macrocycle with one picolinate and two picolyl pendant arms, Hno1pa2py, that was found to easily form stable and inert copper(II) complexes as well; additionally, it resulted in very efficient radiolabeling with ^{64}Cu.[26]

dx.doi.org/10.1021/ic500491c | Inorg. Chem. 2014, 53, 5269−5279

With the above criteria in mind, we decided to investigate the combination of the inertness of cross-bridged macrocycles with the fast and strong chelation properties arising from picolinate moieties. In the current work, a new cross-bridged cyclam derivative with a single picolinate pendant arm, H**cb-te1pa**, is presented along with a thorough study of its complexation properties with Cu^{2+} and Zn^{2+} metal ions.

RESULTS AND DISCUSSION

Synthesis of Hcb-te1pa and Its Copper(II) Complex. The synthetic protocol used for the preparation of H**cb-te1pa** is described in Scheme 1 and consists of two steps starting from

Scheme 1. Synthesis of cb-te1pa[a]

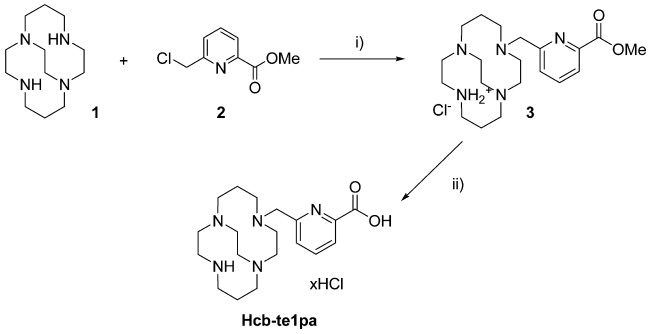

[a](i) CH_3CN, rt, 12 h; (ii) 6 M HCl, reflux, 12 h.

the previously described cross-bridged cyclam **1**[27] and 6-chloromethylpyridine methyl ester **2**.[28] Alkylation of the constrained cyclam with the electrophilic derivative in the absence of a base afforded compound **3** with a 92% yield. This selective mono-N-functionalization of the macrocycle is due to the proton sponge behavior of the cross-bridged cyclam precursor. In fact, the proton produced by the first alkylation induces the protonation of the macrocycle, which prevents the second alkylation from taking place. Thus, the reaction mainly leads to the monoalkylated product, which can be easily isolated using flash chromatography. This ester derivative was subsequently hydrolyzed with an aqueous 6 M HCl solution, leading quantitatively to H**cb-te1pa** in its hydrochloride salt form.

Elution of H**cb-te1pa** through an ion-exchange resin with 0.1 M $HClO_4$ and subsequent slow evaporation of the eluted solution gave single crystals of H_3**cb-te1pa**$(ClO_4)_2$ suitable for X-ray diffraction analysis. An ORTEP view of the structure is shown in Figure 1, and relevant crystallographic data for H_3**cb-te1pa**$(ClO_4)_2$ are collected in Table 6 of the Experimental Section.

The crystal data analysis showed that the macrocycle is protonated on the trans N1 and N3 nitrogen atoms, (Figure 1). This is not surprising because the presence of the cross-bridge results in a structure that brings N2 and N4 within a relatively short distance (2.92 Å in H_3**cb-te1pa**$(ClO_4)_2$), whereas the N1···N3 distance is considerably longer (3.89 Å). Thus, protonation at N1 and N3 reduces the electrostatic repulsion between the ammonium groups of the macrocycle. These protonated nitrogen atoms, N1 and N3, are involved in hydrogen bonds with the remaining two nitrogen atoms of the cyclam fragment: N1−H1, 0.93 Å; N4···H1, 1.95 Å; N1···N4, 2.736(5) Å; N1−H1···N4, 140.7°; N3−H3D, 0.92 Å; N2···H3D, 2.02 Å; N3···N2, 2.766(6) Å; and N3−H3D···N2, 155.6°.

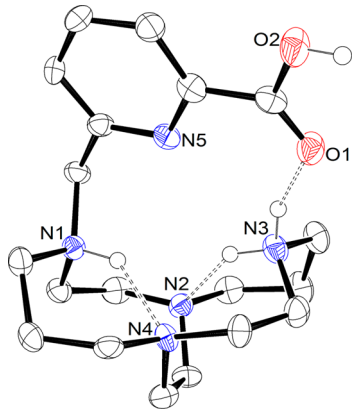

Figure 1. View of the X-ray crystal structure of H_3**cb-te1pa**$(ClO_4)_2$. Perchlorate anions and hydrogen atoms bound to carbon atoms are omitted for clarity. The ORTEP plot is at the 30% probability level.

These hydrogen bonds are probably responsible for the high basicity of the ligand that results in a proton sponge behavior (see below). Similar hydrogen-bonding patterns have been previously observed for diprotonated cross-bridged cyclam derivatives.[19] The N3 nitrogen atom is also involved in intramolecular hydrogen-bond interactions with the O1 oxygen atom of the carboxylic acid group [N3−H3C, 0.92 Å; O1···H3D, 1.92 Å; N3···O1, 2.782(5) Å; and N3−H3D···O1, 155.6°], resulting in the formation of a pseudomacrotricyclic cavity.

The synthesis of the copper(II) complex was performed by reaction of H**cb-te1pa** with $Cu(ClO_4)_2{\cdot}6H_2O$ in aqueous solution at pH ≈ 7, providing the desired complex as the corresponding perchlorate salt in good yield (83%). The mass spectra (ESI^+) showed only one intense peak corresponding to the $[Cu($**cb-te1pa**$)]^+$ entity, thereby confirming the exclusive formation of the desired complex. Single crystals of the Cu^{2+} complex were obtained by slow evaporation of a concentrated aqueous solution at neutral pH. However, despite many efforts and the isolation of several single crystals, it was not possible to obtain suitable crystallographic data for publication. The view of the structure obtained and a brief description are given in the Supporting Information (Figure S1 and Table S1).

Acid−Base Properties of Hcb-te1pa. The protonation constants of H**cb-te1pa** were determined in aqueous solution at 25 °C. The compound has six basic centers consisting of the five nitrogen atoms and the carboxylate function, from which only two could be accurately determined by potentiometric titrations (Table 1). The proton sponge behavior of cross-bridged tetraaza macrocyclic compounds is well-known[12,29−33] and results in very high values of the first protonation constant. For H**cb-te1pa**, such behavior was verified using a ^1H NMR spectroscopic titration in D_2O in the basic pH range (Figure S2, Supporting Information). Although there are marked resonance shifts in the range of pD 8−12, corresponding undoubtedly to the second protonation constant of the compound (see below), there are no shifts in the resonances in the range of pD 12−14, and minor shifts start to become visible only above pD 14. It is thus clear that only at pD > 14 does the last deprotonation step take place. However, the spectroscopic data obtained at the highest pH values do not allow for the determination of the first protonation constant, as only the beginning of the deprotonation process was detected. This equilibrium at very high pH values must correspond to the protonation of one of the

dx.doi.org/10.1021/ic500491c | Inorg. Chem. 2014, 53, 5269−5279

Table 1. Overall (β_i^H) and Stepwise (K_i^H) Protonation Constants, in log Units, for Hcb-te1pa and Related Compounds at 25.0 °C in 0.10 M KNO_3

equilibrium reaction[a]	L = **cb-te1pa**$^{-b}$	L = te1pa^{-c}	L = cb-cyclam[d]
	log β_i^H		
$L + H^+ \rightleftarrows HL$	[e]	11.55	12.42
$HL + H^+ \rightleftarrows H_2L$	10.13(5)		
$L + 2H^+ \rightleftarrows H_2L$		21.66	22.61
$HL + 2H^+ \rightleftarrows H_3L$	12.56(5)		
$L + 3H^+ \rightleftarrows H_3L$		24.37	(20.23)
$HL + 3H^+ \rightleftarrows H_4L$	<14.56		
$L + 4H^+ \rightleftarrows H_4L$		26.07	24.00
	log K_i^H		
$L + H^+ \rightleftarrows HL$	[e]	11.55	12.42
$HL + H^+ \rightleftarrows H_2L$	10.13	10.11	10.20
$H_2L + H^+ \rightleftarrows H_3L$	2.43	2.71	
$H_3L + H^+ \rightleftarrows H_4L$	<2.0	1.7	1.39

[a]L denotes the ligand in general; charges are omitted for simplicity. [b]Values in parentheses are standard deviations in the last significant figure. [c]From ref 24. [d]From ref 34, with I = 0.1 M in KCl. [e]This protonation constant could not be experimentally determined.

macrocyclic amines and should be highly influenced by hydrogen-bonding interactions, as seen in the single-crystal X-ray diffraction structure of H_3**cb-te1pa**$(ClO_4)_2$ described above. The second and third protonation constants of H**cb-te1pa** were determined by conventional potentiometric titrations in aqueous solution at 0.10 M KNO_3 ionic strength. The second constant (log K_2 = 10.13) must correspond to the protonation of a second macrocyclic amine in the opposite position in order to minimize the electrostatic repulsion, whereas the third one (log K_3 = 2.43) should correspond to protonation of the carboxylate group. No other protonation constants could be calculated, meaning that additional protonation equilibria may happen only at pH < 2.

Thermodynamic Stability of the Metal Complexes of Hcb-te1pa. The stability constants of the complexes formed by H**cb-te1pa** with Cu^{2+} and Zn^{2+} ions were also determined by potentiometric titrations in aqueous solution under the same experimental conditions as those used in the protonation experiments (Table 2). The equilibrium of formation of the copper(II) and especially the zinc(II) complexes is somewhat slow in the acidic pH range. For the Cu^{2+} cation, the complexation is almost complete at low pH but is relatively slow up to pH 4. To overcome this double problem, conventional titrations were performed starting from pH values slightly below 2 in order to observe a significant percentage of free metal ion (at least 18%), thus allowing for the determination of the corresponding stability constant while giving the solution enough time to reach the equilibrium prior to the start of the titration. During titrations, each experimental point included a supplementary equilibration time in order to obtain fully stabilized measurements (see the Experimental Section). For the Zn^{2+} ion, there is essentially no complexation below pH 4, and in the range of pH 4−6, the complexation is extensive but very slow, taking up to 1 week to reach the final equilibrium. For this reason, batch titrations were prepared in the range of pH 4−6 and were left to equilibrate until full stabilization, whereas conventional titrations were used in the remaining pH regions.

The speciation is quite simple with both Cu^{2+} and Zn^{2+} cations; the fully deprotonated complex is the only species in the intermediate pH range, whereas hydroxocomplexes can be found at basic pH (Figure S3, Supporting Information). For a correct comparison of the thermodynamic stability of the complexes of H**cb-te1pa** with the corresponding values of other ligands from the literature, the pM values (pM = −log $[M^{n+}]$) that take into account the different basicity properties of the various ligands[35] were also calculated (Table 3). Both the stability constants obtained and the pM values calculated demonstrate the very high thermodynamic stability of the

Table 2. Overall (β_{MH_iL}) and Stepwise (K_{MH_iL}) Stability Constants, in log Units, For Complexes of Hcb-te1pa and Related Ligands with Cu^{2+} and Zn^{2+} Cations at 25.0 °C in I = 0.10 M KNO_3

equilibrium reaction[a]	L = **cb-te1pa**$^{-b}$	L = te1pa^{-c}	L = cb-cyclam[d]
	log β_{MH_iL}		
$Cu^{2+} + HL \rightleftarrows CuL + H^+$	11.00(5)		
$Cu^{2+} + HL \rightleftarrows CuLH_{-1} + 2H^+$	0.95(9)		
$Cu^{2+} + L \rightleftarrows CuL$		25.5	27.1
$Cu^{2+} + H^+ + L \rightleftarrows CuHL$		27.67	
$Cu^{2+} + L \rightleftarrows CuLH_{-1} + H^+$		14.35	
$Zn^{2+} + HL \rightleftarrows ZnL + H^+$	3.83(3)		
$Zn^{2+} + HL \rightleftarrows ZnLH_{-1} + 2H^+$	−7.50(4)		
$Zn^{2+} + L \rightleftarrows ZnL$		18.86	
$Zn^{2+} + H^+ + L \rightleftarrows ZnHL$		21.38	
$Zn^{2+} + L \rightleftarrows ZnLH_{-1} + H^+$		7.84	
	log K_{MH_iL}		
$Cu^{2+} + L \rightleftarrows CuL$		25.5	27.1
$CuL + H^+ \rightleftarrows CuHL$		2.17	
$CuLOH + H^+ \rightleftarrows CuL$	10.05	11.15	
$Zn^{2+} + L \rightleftarrows ZnL$		18.86	
$ZnL + H^+ \rightleftarrows ZnHL$		2.52	
$ZnLOH + H^+ \rightleftarrows ZnL$	11.33	11.02	

[a]L denotes the ligand in general, and for H**cb-te1pa**, HL needs to be considered because the last deprotonation occurs only with complexation; charges of ligand and complex species are omitted for simplicity. [b]Values in parentheses are standard deviations in the last significant figure. [c]From ref 24. [d]From ref 34 by spectrophotometric competition without an ionic strength control.

dx.doi.org/10.1021/ic500491c | Inorg. Chem. 2014, 53, 5269−5279

Table 3. Calculated pM Values for the Complexes of Hcb-te1pa and Related Compounds[a]

cation	Hcb-te1pa[b]	Hte1pa[c]	cb-cyclam[d]
Cu^{2+}	15.67	18.64	19.29
Zn^{2+}	8.50	12.00	

[a]Values calculated at pH 7.4 for a 100% excess of ligand with $[M^{2+}]_{tot} = 1.0 \times 10^{-5}$ M, based on the reported stability constants. [b]This work. [c]From ref 24. [d]From ref 34.

copper(II) complex of H**cb-te1pa**. Importantly, they also show a very high selectivity of H**cb-te1pa** for copper(II) complexation over zinc(II). Although the two other ligands taken for comparison exhibit larger pCu values, the one obtained for the copper(II) complex of H**cb-te1pa** is still high enough for a strong coordination of Cu^{2+} as well as to potentially prevent transchelation. However, the thermodynamic stability is not the only important criterion to determine the efficiency of metal complexation, as other factors, such as kinetic inertness or in vivo stability, are possibly more important with regard to the potential applications of this complex.

DFT Calculations. Despite the absence of an acceptable solution for the refinement of the crystallographic data of the copper(II) complex of H**cb-te1pa**, the basic structure of the complex with the positions of the copper(II) ion and the ligand atoms could be established. Aiming to obtain information on the structure of this complex, we performed DFT calculations in aqueous solution (PCM model) at the TPSSh/TZVP level. Geometry optimization provided the structure shown in Figure 2, which also gives bond distances of the metal coordination environment.

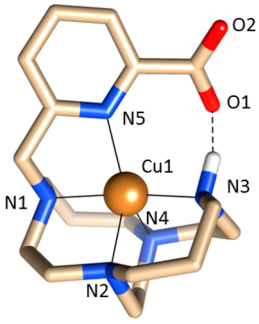

Figure 2. Structure of the $[Cu(\textbf{cb-te1pa})]^+$ complex cation obtained with DFT calculations at the TPSSh/TZVP level. Hydrogen atoms bonded to carbon atoms are omitted for clarity. Bond distances (Å) are as follows: Cu1–N1, 2.045; Cu1–N2, 2.164; Cu1–N3, 2.018; Cu1–N4, 2.151; and Cu1–N5, 2.165.

The metal ion in $[Cu(\textbf{cb-te1pa})]^+$ is five-coordinate, being directly bound to the four nitrogen atoms of the macrocyclic unit and the nitrogen atom of the pyridyl group. The distance between the metal atom and the oxygen atom of the carboxylic group O(1) [3.24 Å] is too long to be considered as a bond distance. The coordination polyhedron around the copper center can be defined as a trigonal bipyramid in which the equatorial plane is defined by the N atoms of the cyclam fragment N2 and N4, the nitrogen atom of the pyridyl unit N5, and the metal ion and the apical positions are defined by donor atoms N1 and N3. Alternatively, the coordination polyhedron may be defined as square pyramidal, where the basal plane is delineated by N1, N2, N3, and N5 and the apical position is defined by N4. The index of trigonality, τ, was calculated to be 0.58, which points to a distorted coordination polyhedron that is half-way between the two ideal geometries ($\tau = 0$ for a perfect square-pyramidal geometry and $\tau = 1$ for an ideal trigonal-bipyramidal geometry).[36]

The cyclam unit presents a cis-V-folded coordination configuration[37] that provides four convergent nitrogen donor atoms for Cu^{2+} coordination. The bicyclo[6.6.2] ligand backbone shows a [2323]/[2323] conformation.[38] Interestingly, the diprotonated form of the ligand (see above) adopts the same conformation. An intramolecular hydrogen-bonding interaction exists between the NH group of the macrocyclic fragment and one of the oxygen atoms of the carboxylate function [N(3)···O(1), 2.689 Å; N(3)–H(3)···O(1), 1.709 Å; and N(3)–H(3)···O(1), 155.9°], which results in the formation of a macrotricyclic-like structure because of the formation of a third pseudomacrocycle.

Spectroscopic Study of the Complexes. UV–vis–NIR absorption spectra of the copper(II) complex of H**cb-te1pa** were recorded in aqueous solution at 25 °C in the pH 2–10 range. The complex demonstrated no pH dependence, as all recorded spectra are perfectly identical. The spectra exhibit a very intense band around 272 nm because of the presence of the picolinate chromophore,[39] with a shoulder at 305 nm corresponding to a charge transfer band, probably a LMCT transition from amine donors to the metal center, an intense d–d transition band at 600 nm, and a slightly less intense band at 938 nm (Figure S4, Supporting Information). The position and intensity of the bands exclude regular octahedral or tetragonal geometries. However, because of the plasticity of copper(II), it is difficult to infer structural features from these data alone.[40,41]

To gain more structural information, the X-band EPR spectra of frozen aqueous samples of the copper(II) complex around neutral pH were acquired at 90 K. The spectra showed the presence of a single paramagnetic species, and no superhyperfine splitting resulting from coupling with the nitrogen atoms of the ligand was observed (Figure 3). Spectroscopic absorption data, hyperfine coupling constants A_i ($i = x, y$, and z), and g values obtained by EPR spectra simulation[42] are compiled in Table 4. These data clearly show a distortion from axial symmetry, and three different values of g were obtained, with $g_x > g_y \gg g_z \approx 2.00$. These data, together with the values of the hyperfine splitting parameters, are indicative of a

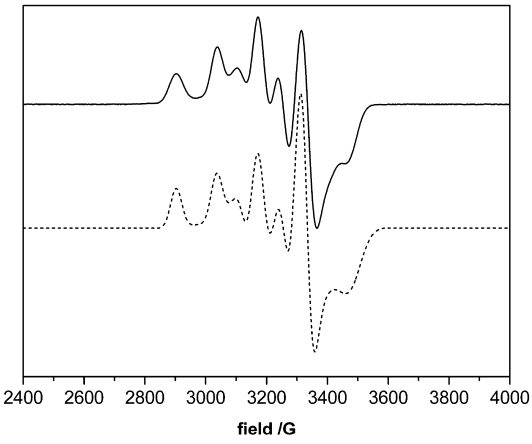

Figure 3. Experimental (solid) and simulated (dashed) X-band EPR spectrum of the copper(II) complex of H**cb-te1pa** recorded in frozen aqueous solution.

dx.doi.org/10.1021/ic500491c | Inorg. Chem. 2014, 53, 5269–5279

Table 4. Spectroscopic Parameters for the Copper(II) Complexes of Hcb-te1pa and Related Ligands in Neutral Aqueous Solution

complex	pH	UV−vis−NIR λ_{max} (ε)[a]	EPR parameters[b]					
			g_x	g_y	g_z	A_x	A_y	A_z
[Cu(**cb-te1pa**)]$^+$	7.5	272 (8852), 305 (4257), 600 (234), 938 (152)	2.192	2.108	1.987	136.3	68.1	37.7
[Cu(te1pa)]$^{+c}$	~7.5	268 (11 571), 556 (197)	2.036	2.041	2.184	1.6	44.7	188.5
[Cu(dbf-cb-do2a)][d]	8.9	650 (86), 1051 (57)	2.211	2.117	2.007	115.9	51.0	75.4

[a]At 25 °C; λ_{max}, nm; ε, M^{-1} cm^{-1}. [b]In frozen solution at 90 K, A_i is given in 10^{-4} cm^{-1}. [c]From ref 24. [d]From ref 12.

predominance of the d_z^2 ground state that is characteristic of axially compressed geometries such as distorted compressed octahedral or trigonal bipyramidal.[40,41,43−47] Although the compressed octahedral and trigonal bipyramidal geometries cannot be distinguished in solution by their EPR spectra, they present very different bands in the vis−NIR spectra that generally also differ in intensity. Indeed, the vis−NIR spectra of copper(II) complexes in trigonal bipyramidal geometry have more intense bands than those of compressed octahedral ones, but the latter complexes present a NIR band of the same intensity as that of the vis region that is separated by more than 5.0 kK, whereas that of the distorted trigonal bipyramidal stereochemistry involves a single peak in the visible region that tails into the NIR.[46−48] In the case of the [Cu(**cb-te1pa**)]$^+$ complex cation, the NIR band is somewhat less intense than the one in the visible region, which suggests that a combination of the two geometries is occurring in solution, the trigonal bipyramidal and the compressed octahedral geometries, as explained below. A very similar geometry was found for the cross-bridged cyclen derivative [Cu(dbf-cb-do2a)] in solution and in the solid state[12] (Table 4).

The structure found for the [Cu(**cb-te1pa**)]$^+$ complex in the crystal (see DFT calculations) differs from that observed in solution because in the solid state one coordination position is missing in the equatorial plane, meaning that a trigonal bipyramidal geometry with compressed axial distances was found instead. Different attempts to obtain an optimized geometry of the complex (with DFT calculations) in which an oxygen atom of the carboxylate group is coordinated to the metal ion were unsuccessful. This indicates that an oxygen atom of the ligand is most likely involved in a hydrogen bond with the NH group of the ligand. Thus, in solution, the fourth position on the equatorial plane of the compressed distorted octahedral geometry is most likely occupied by a water molecule, which is in line with the formation of the weak monohydroxocomplex evidenced by pH−potentiometric titrations. This indicates that the water molecule bound to the copper center that is completing the equatorial plane of the distorted compressed octahedral geometry of the complex is weakly bound to the metal center and that in solution an equilibrium between trigonal bipyramidal and distorted compressed octahedral geometries exists.

The ^{1}H and ^{13}C NMR spectra of the [Zn(**cb-te1pa**)]$^+$ complex were obtained in D_2O solution at pD 6.8 and 298 K. The proton spectrum consists of 29 signals, which points to a C_1 symmetry of the complex in solution. This is also confirmed by the ^{13}C NMR spectrum, which shows one peak for each of the 19 carbon nuclei of the ligand backbone. Both the ^{1}H and ^{13}C NMR spectra remain unchanged in the temperature range 5−70 °C, which highlights the rigidity of the complex in solution (Figures S5 and S6, Supporting Information). The ^{1}H NMR spectrum shows the expected three signals resulting from the proton nuclei of the pyridyl moiety at 7.62, 7.74, and 8.14 ppm, whereas the protons of the CH_2 group bound to the pyridyl fragment give an AB pattern with ^2J = 18 Hz in which the larger shift for the equatorial proton results from the combined deshielding effects of the pyridyl ring current and the polarizing effect of the Zn^{2+} ion on the C−H bond pointing away from it.[49] The ^{1}H NMR signal resulting from NH protons is observed at 4.22 ppm as a complicated multiplet because of coupling with the four CH_2 protons at a three-bond distance. As previously observed for different metal complexes with secondary polyamines, the NH protons exchange very slowly with D_2O at about neutral pH.[50] Increasing the temperature increases the exchange rate of these protons with D_2O such that at 70 °C the signal resulting from the NH group is not observed.

Formation and Dissociation of the Copper(II) Complex. It is known that cross-bridged tetraaza macrocycles usually form kinetically stable copper(II) complexes, especially those appended with coordinating arms such as acetate.[1,4,5] Indeed, some of the recently reported ligands of this type yield copper(II) complexes that are among the most inert described so far with regard to acid-assisted dissociation, such as the complexes of H_2c3b-do2a,[10] H_2c3b-te2a,[11] and H_2dpe-do2a.[12] However, one of the main drawbacks of cross-bridged ligands is their generally unfavorable and slow complexation reaction with metal cations, which is largely because of the difficulty in displacing the last proton of the free ligands that arises from their very high basicity and because of the conformational hindrance posed by the rigidity of the ligand structure.[29,31,51] Because a rapid formation of the copper(II) complex is essential for its use in radiopharnaceuticals, some of the most inert cross-bridged complexes may be useless for these applications given the rather harsh conditions (typically very high temperature and/or high pH) required to achieve near quantitative metal complexation, which are impractical when working with most of the radioisotopes used in medicine. It was previously found that appending a single picolinate arm on cyclen and cyclam macrocycles results in a somewhat surprisingly fast complexation of copper(II),[24] and it was expected that the same effect could be obtained with the ethylene cross-bridged cyclam counterpart. Thus, the copper(II) complex formation of H**cb-te1pa** was followed spectroscopically over time in different buffered solutions from acidic to neutral pH. In an equimolar metal-to-ligand ratio, complex formation is instantaneous at physiological pH (7.4) and is extremely fast at pH 5: it is complete (>99%) within a few seconds in the former case and within ca. 3 min in the latter (Figure S7, Supporting Information). The reaction becomes progressively slower under increasingly acidic conditions, enabling a kinetic study under pseudo-first-order conditions using conventional UV−vis spectroscopic methods. Such a kinetic study was performed at pH 3, which is at the lower limit of the pH range in which the copper(II) complexation is approximately complete under equilibrium in equimolar metal-

dx.doi.org/10.1021/ic500491c | Inorg. Chem. 2014, 53, 5269−5279

to-ligand conditions. The data obtained for this reaction under pseudo-first-order conditions, using 10 equiv. of metal cation in excess of the ligand, resulted in a formation half-time ($t_{1/2}$) of 1.7 min and showed that the formation is quantitative (>99%) within ca. 10 min. This behavior can be rationalized by analyzing the preorganized structure of the ligand (see its crystallographic structure described earlier). This conformation is favored by a hydrogen bond between the carboxylic acid function of the picolinate and the sole secondary amine of the macrocycle. The nitrogen atom of the picolinate arm is located just outside the macrocyclic pocket in perfect position for copper(II) coordination. According to these results, H**cb-te1pa** is, to the best of our knowledge, the cross-bridged ligand endowed with the fastest complexation ability for copper(II) under very mild reaction conditions. Two other cross-bridged cyclam derivatives containing one or two methylenephosphonate pendant arms, H_3cb-te1a1p and H_4cb-te2p, were previously found to form copper(II) complexes readily in aqueous solution,[18] but their reported behavior seems to be somewhat less favorable than that of ours.

The slow dissociation of the complexes is probably the most important feature to be evaluated for selection of compounds to be used in medical applications.[1,4,5] The kinetics of acid-assisted dissociation of the copper(II) complex of H**cb-te1pa** was studied under pseudo-first-order conditions in acidic aqueous solutions. The dissociation was monitored by following the changes in the visible absorption band of the complex at 25 °C in 5 M $HClO_4$ or at 20, 25, 37, 60, and 90 °C in 5 M HCl. The half-life values determined are collected in Table 5 together with literature values for related compounds.

Table 5. Acid-Assisted Dissociation Inertness for the Copper(II) Complexes of Hcb-te1pa and Selected Literature Ligands

ligand	conditions	half-life ($t_{1/2}$)	ref
H**cb-te1pa**	5 M HCl, 90 °C	0.7 min	this work
	5 M HCl, 60 °C	10.4 min	this work
	5 M HCl, 37 °C	111 min	this work
	5 M HCl, 25 °C	465 min	this work
	5 M HCl, 20 °C	946 min	this work
	5 M $HClO_4$, 25 °C	96 days	this work
H_2c3b-do2a	12 M HCl, 90 °C	1.1 days	10
H_2c3b-te2a	12 M HCl, 90 °C	>7 days	11
H_2dpe-do2a	12 M HCl, 90 °C	30.8 days	12
H_2cb-te2a	12 M HCl, 90 °C	96 min	52
	5 M HCl, 90 °C	9240 min	52
H_2dbf-do2a	5 M HCl, 90 °C	258.8 min	12
H_3cb-te1a1p	5 M HCl, 90 °C	408 min	18
H_4cb-te2p	5 M HCl, 90 °C	228 min	19
cb-cyclam	5 M HCl, 90 °C	11.8 min	53
H_2cb-do2a	5 M HCl, 30 °C	<2 min	52
cyclam	5 M HNO_3, 25 °C	20.9 min	54, 55
Hno1pa2py	3 M HCl, 90 °C	204 min	26
Hdo1pa	2 M HCl, 25 °C	1.4 min	24
Hte1pa	1 M HCl, 25 °C	32 min	24

The marked difference between the half-life values in $HClO_4$ and HCl media, which, in our case, was found to be very significant at 25 °C, has been generally explained by the important role that anions sometimes play in the dissociation mechanism.[56] However, the overall very good half-life values obtained for the copper(II) complex of H**cb-te1pa** are more important. Although an important decrease of the kinetic inertness was found for higher temperatures, the half-life time of the complex is still of about 2 h at 37 °C in 5 M HCl. The experimental kinetic data at variable temperature also allowed the temperature dependence of the observed rate constants to be obtained from fitting to the Arrhenius equation (Figure S8, Supporting Information). Compared to the reported copper(II) complexes of nonconstrained macrocyclic chelators, the copper(II) complex of H**cb-te1pa** exhibits a higher inertness. For instance, when compared directly to its nonconstrained analogue Hte1pa, the gain provided by the ethylene bridge at 25 °C is from a half-life time of 32 min in 1 M HCl to 465 min in 5 M HCl for the complex now reported. This inertness is also higher than that measured for H_2cb-do2a, whereas the measured half-life times of our complex are shorter than those reported in the literature for other ansa- or cross-bridged macrocycles such as H_2dpe-do2a, H_2c3b-te2a, H_3cb-te1a1p, and, especially, H_2cb-te2a. Therefore, there is sufficient inertness for potential in vivo applications of H**cb-te1pa**, especially when the key advantage presented by its fast complexation process is taken into consideration.

Electrochemistry of the Copper(II) Complex. The reduction of copper(II) to copper(I) of the macrocyclic complex in biological media followed by the demetalation of the complex is one of the explanations for the observed dissociation of some copper(II) complexes of macrocyclic ligands.[52] It is thus important to ensure the electrochemical inertness as well as the reversibility of the redox system. To determine the redox behavior of the complex of H**cb-te1pa**, cyclic voltammetry assays were performed in aqueous solution at pH values of 2.3 and 6.8 (Figure 4). The experiments were carried out with a glassy carbon working electrode in solutions containing 0.1 M $NaClO_4$ as the supporting electrolyte. At neutral pH, a quasi-reversible system at $E_{1/2}$ = −0.86 V_{SCE} (ΔE_p = 160 mV) was observed with a negligible oxidation peak of free Cu^+ ions to Cu^{2+} at 0 V_{SCE}. This study indicates that the complex is quite stable on the CV time scale even though a small demetalation phenomenon can be observed. Furthermore, the reduction process observed for the copper(II)

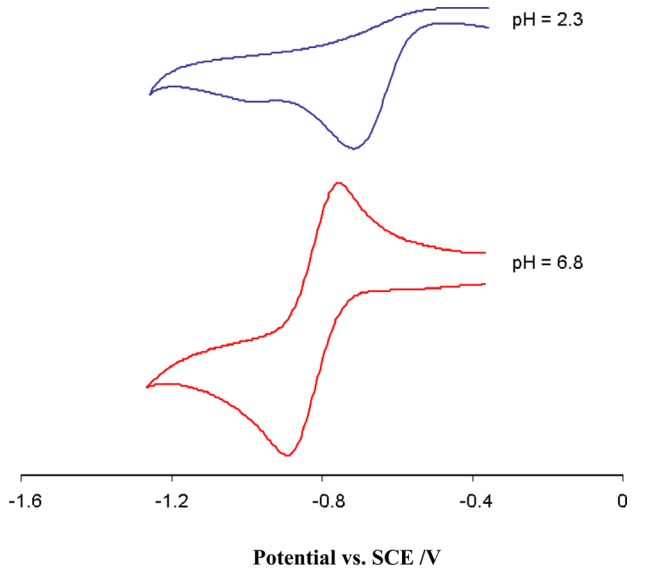

Figure 4. Cyclic voltammograms of the copper(II) complex of H**cb-te1pa** recorded at different pH values (scan rate, 100 mV/s).

dx.doi.org/10.1021/ic500491c | Inorg. Chem. 2014, 53, 5269−5279

complex of **Hcb-te1pa** (E_{pc} = −0.696 V versus NHE upon conversion) is well below the estimated −0.400 V (NHE) threshold for typical bioreductants,[4] which augurs well for the possible redox inertness of the complex in biological media. In contrast, in acidic media (pH 2.3), the Cu^{2+}/Cu^{+} system becomes irreversible. The reduction of Cu^{2+} ions to Cu^{+} can be observed at E_{pc} = −0.77 V_{SCE}, whereas reoxidation cannot. A high oxidation current appears at 0.13 V_{SCE} because of the oxidation of free Cu^{+} to Cu^{2+}. At this pH, the complex is not stable at all, and demetalation occurs.

CONCLUSIONS

Because of their commercial availability and versatile properties, dota-like macrocycles (cyclen-based ligands bearing acetate pendant arms) are still among the most used copper(II) chelators in bioapplications including PET imaging. However, it is now well-recognized that they do not meet the strict specifications for applications in nuclear medicine, especially in terms of their in vivo inertness. Some recently prepared chelating agents, such as the constrained cb-te2a, represent a significant improvement relative to conventional macrocyclic chelators. However, the slow kinetics of their metal complex formation still constitutes a serious drawback that justifies the continuation of research in this area. With this in mind, we have recently reported the very promising properties of monopicolinate cyclam Hte1pa for complexation of Cu^{2+} and $^{64}Cu^{2+}$, but the need to improve its inertness was evident. In the present work, the synthesis of the cross-bridged analogue of Hte1pa was achieved in high yield using a rapid synthetic route based on the proton sponge properties of the macrocycle. The new compound conveniently combines the inertness of the cross-bridged macrocycles with the fast and strong chelation properties brought by the picolinate pendant arm. Indeed, it presents a very fast complexation of copper(II) at neutral and moderately acidic pH. The proton sponge behavior of the constrained ligand was demonstrated using both NMR and potentiometric investigations. The X-ray structure of the triprotonated ligand clearly showed that the ligand is preorganized for metal complexation even in acidic medium.

The potentiometric studies confirmed the high thermodynamic stability of the copper(II) complex and the very high selectivity for Cu^{2+} over Zn^{2+}. The synthesis of the copper(II) complex was achieved, and the coordination geometry of the copper center in the complex was established in solution from UV−vis and EPR spectroscopies. In solution, there appears to exist an equilibrium between a trigonal bipyramidal geometry and a Jahn−Teller distorted compressed octahedral coordination environment where the last coordination position of the equatorial plane is occupied by a weakly bound water molecule. The inertness of the copper(II) complex was studied in different media and showed long half-life values when it was compared to a list of copper(II) complexes of similar chelates. Cyclic voltammetry studies also proved the inertness of the copper(II) complex toward redox-assisted demetalation.

The presence of the ethylene cross-bridge thus leads to an improvement of the chelator properties when compared to the previously studied nonbridged analogue Hte1pa. The **Hcb-te1pa** ligand appears to be a very promising copper(II) chelator and an attractive alternative to the H_4dota or H_2cb-te2a macrocycles for the development of new radiopharmaceuticals. Consequently, **Hcb-te1pa** could be grafted on biomolecules in order to prove its use in either immuno-PET or RIT. This can be achieved either by N-functionalization via the free secondary amine group or by C-functionalization on a carbon atom of the macrocycle or the aromatic ring. Such efforts are currently in progress.

EXPERIMENTAL SECTION

Materials and Methods. Reagents were purchased from ACROS Organics and from Aldrich Chemical Co. Cross-bridged cyclam **1** was purchased from CheMatech (Dijon, France), and 6-chloromethylpyridine-2-carboxylic acid methyl ester **2**[28] was synthesized as previously described. Elemental analyses were performed at the Service de Microanalyse, CNRS, 69360 Solaize, France. NMR and Mass spectra were recorded with an Autoflex MALDI TOF III smartbeam spectrometer or with ESI on a Shimadzu LCMS-2020 spectrometer. The HR-MS analyses were performed at the Institute of Analytic and Organic Chemistry, ICOA in Orleans.

Syntheses. *Compound 3.* A solution of 6-chloromethylpyridine-2-carboxylic acid methyl ester **2** (0.180 g, 0.97 mmol) in 25 mL of distilled acetonitrile was added to a solution of cross-bridged cyclam **1** (0.200 g, 0.88 mmol) in 175 mL of distilled acetonitrile. The mixture was stirred overnight at rt. After evaporation of the solvent, the crude product was purified by column chromatography in silica gel ($CHCl_3$/MeOH 8:2) to yield compound **3** as a colorless oil (0.305 g, 92%). ^{1}H NMR ($CDCl_3$, 400 MHz): 0.95−1.06 (m, 1H), 1.41−1.55 (m, 1H), 1.58−1.70 (m, 1H), 1.83−1.94 (m, 1H), 2.33−2.64 (m, 8H), 2.65−2.79 (m, 3H), 2.80−2.93 (m, 4H), 2.93−3.06 (m, 3H), 3.12−3.22 (m, 1H), 3.46 (d, ^2J = 13.2 Hz, 1H), 3.48−3.59 (m, 1H), 3.92 (s, 3H), 4.08 (d, ^2J = 12.8 Hz, 1H), 7.52 (d, ^3J = 7.6 Hz, 1H), 7.90 (dd, ^3J = 8.0, 7.6 Hz, 1H), 7.98 (d, ^3J = 8.0 Hz, 1H). ^{13}C NMR ($CDCl_3$, 100 MHz): 20.5, 25.2, 43.4, 45.7, 48.6, 50.6, 51.0, 52.0, 52.2, 52.3, 54.4, 54.9, 55.9, 62.7, 123.2, 127.9, 138.2, 145.5, 157.8, 164.1. MALDI-TOF (dithranol): m/z = 376.25 (M + 1). Anal. Calcd for $C_{20}H_{33}N_5O_2\cdot HCl\cdot 2H_2O$: C, 53.62; H, 8.55; N, 15.63%. Found: C, 53.62; H, 8.69; N, 15.35%.

Hcb-te1pa. Hydrochloric acid (20 mL, 6 M) was slowly added to compound **3** (0.610 g, 1.62 mmol), and the mixture was refluxed overnight. After cooling to rt, the solvent was evaporated to yield H**cb-te1pa**·4.5HCl·$3H_2O$ as an off-white solid in quantitative yield. ^{1}H NMR (D_2O, 400 MHz): 1.60 (d, ^2J = 17.2 Hz, 1H), 1.79 (d, ^2J = 16.4 Hz, 1H), 2.34−2.51 (m, 2H), 2.59−2.76 (m, 4H), 2.85−2.91 (m, 2H), 3.10−3.70 (m, 13H), 4.02 (dt, ^3J = 7.6 Hz, ^4J = 4.4 Hz, 1H), 4.17 (d, ^2J = 13.6 Hz, 1H), 5.02 (d, ^2J = 14.0 Hz, 1H), 7.84 (d, ^3J = 7.6 Hz, 1H), 8.17 (dd, ^3J = 8.0, 7.6 Hz, 1H), 8.34 (d, ^3J = 8.0 Hz, 1H). ^{13}C NMR ($CDCl_3$, 100 MHz): 20.8, 21.1, 44.9, 49.9, 51.8, 52.2, 52.7, 56.3, 57.2, 58.1, 59.3, 60.5, 61.1, 129.5, 133.2, 143.0, 151.3, 154.0, 171.7. MALDI-TOF (dithranol): m/z = 362.23 (M + 1). Anal. Calcd for $C_{19}H_{31}N_5O_2\cdot 5HCl\cdot 4.5H_2O$: C, 36.52; H, 7.26; N, 11.21%. Found: C, 36.79; H, 7.22; N, 10.93%.

Caution! *Although no problem arose during our experiments, salts of perchlorate and their metal complexes are potentially explosive and should be handled with great care and in small quantities.*[57]

*Preparation of [Cu(**cb-te1pa**)]ClO_4.* $Cu(ClO_4)_2\cdot 6H_2O$ (0.070 g, 0.19 mmol) was added to a solution of H**cb-te1pa**·4.5HCl·$3H_2O$ (0.100 g, 0.17 mmol) in 10 mL of water, and the pH was adjusted to ≈7 with an aqueous KOH solution. The mixture was heated at 80 °C for 2 h and then stirred overnight at rt. Solid impurities were filtered off, and the solution was evaporated to dryness. After addition of acetonitrile, the gray powder was filtered off, and the filtrate was evaporated to yield compound [Cu(**cb-te1pa**)]ClO_4 as a blue powder (0.090 g, 82%). ESI-MS: (CH_3CN/H_2O, 50:50) 423.10 (M^+). ESI-HR-MS (positive, H_2O) m/z calcd. for $C_{19}H_{31}CuN_5O_2$, 212.0881; found, 212.0887 $[M + 2]^{2+}$.

Potentiometric Studies. *Equipment and Work Conditions.* The potentiometric setup has been described before.[26] The titrant was a KOH solution prepared at ca. 0.1 M from a commercial ampule of analytical grade, and its accurate concentration was obtained by application of the Gran's method[58] upon titration of a standard HNO_3 solution. Ligand solutions were prepared at about 2.0 × 10^{-3} M, and the Cu^{2+} and Zn^{2+} solutions were prepared at ca. 0.05 M from analytical grade nitrate salts and standardized by complexometric

dx.doi.org/10.1021/ic500491c | Inorg. Chem. 2014, 53, 5269−5279

titrations with H_4edta (ethylenediaminetetraacetic acid).[59] Sample solutions for titration contained approximately 0.04 mmol of ligand in a volume of 30 mL where the ionic strength was kept at 0.10 M using KNO_3 as the background electrolyte. Metal cations were added at 0.9 equiv of the ligand amount in complexation titrations. Batch titrations were prepared in a similar way but with each titration point corresponding to $^1/_{10}$ of the amount of a conventional titration sample. Batch titration points were incubated in tightly closed vials at 25 °C until potential measurements attained complete stability, which happened within 1 week.

Measurements. All measurements were carried out at 25.0 ± 0.1 °C under an inert atmosphere. The electromotive force of the sample solutions was measured after calibration of the electrodes by titration of a standard HNO_3 solution at 2.0×10^{-3} M under the work conditions. The $[H^+]$ of the solutions was determined by measurement of the electromotive force of the cell, $E = E^{o\prime} + Q \log [H^+] + E_j$. The term pH is defined as $-\log [H^+]$. $E^{o\prime}$ and Q were determined from the acid region of the calibration curves. Deviations from the Nernst law at very low pH (pH < 2.5) were corrected with the VLpH software,[60] which performs a $[H^+]$ correction based on a very low pH calibration procedure. The liquid-junction potential, E_j, was otherwise found to be negligible for pH > 2.5 under the experimental conditions used. The value of $K_w = [H^+][OH^-]$ was found to be equal to $10^{-13.78}$ by titrating a solution of known $[H^+]$ at the same ionic strength in the alkaline pH region, considering $E^{o\prime}$ and Q valid for the entire pH range. Each titration consisted of 80−100 equilibrium points in the pH range of 2.5−11.5 (or 1.5−11.5 for Cu^{2+} complexations), and at least two replicate titrations were performed for each particular system.

Calculations. The potentiometric data were refined with the Hyperquad software,[61] and speciation diagrams were plotted using the HySS software.[62] The overall equilibrium constants β_i^H and $\beta_{M_mH_hL_l}$ are defined by $\beta_{M_mH_hL_l} = [M_mH_hL_l]/[M]^m[H]^h[L]^l$ ($\beta_i^H = [H_hL_l]/[H]^h[L]^l$ and $\beta_{MH_{-1}L} = \beta_{ML(OH)} \times K_w$). Differences in log units between the values of protonated (or hydrolyzed) and nonprotonated constants provide the stepwise (log K) reaction constants ($K_{M_mH_hL_l} = [M_mH_hL_l]/[M_mH_{h-1}L_l][H]$). The errors quoted are the standard deviations calculated by the fitting program from all the experimental data for each system.

Spectroscopic Studies. UV−vis−NIR spectra of the copper(II) complex were measured at 25 °C on Unicam UV4 (UV−vis) or Shimadzu UV3100 (vis−NIR) spectrometers in aqueous solutions of the complex at ca. 0.1 mM in the UV range or ca. 2.0 mM in the vis−NIR range. EPR spectra of the copper(II) complex were measured on a Bruker EMX 300 spectrometer operating in the X-band that was equipped with a continuous-flow cryostat for liquid nitrogen, and measurements were recorded in frozen aqueous solutions (90 K) at 1 mM complex and 1 M $NaClO_4$ at pH 7.5. Selected EPR spectra were simulated with SpinCount software[42] to determine the relevant parameters. ^{1}H and ^{13}C NMR spectra at variable temperatures were recorded with a Bruker Avance 500 (500 MHz) spectrometer. A ^{1}H NMR titration of H**cb-te1pa** was performed in D_2O solution at 298.2 K on a Bruker Avance II+ 400 NMR spectrometer, focusing on the most basic pH range. A ligand sample solution was prepared at ca. 2×10^{-3} M without control of the ionic strength, and the titrant was a freshly prepared CO_2-free KOD solution. Base additions were performed directly in the NMR tube with a micropipet. The pH* was measured with an Orion Star A214 pH/ISE meter fitted with a Hamilton Spintrode PN23819703 combined microelectrode upon calibration with commercial buffers in aqueous solution (pH 12.00, 8.00, and 4.00). The final pD was calculated according to the equation pD = pH* + (0.40 ± 0.02),[63] where pH* corresponds to the reading on the pH meter.

Kinetic Studies. The formation of the copper(II) complex of H**cb-te1pa** was studied in buffered aqueous solutions at 25 °C. The increasing intensity of the complex's d−d transition band in the visible range (600 nm) was followed at pH 5.0 (0.2 M potassium acetate buffer) and pH 7.4 (0.2 M HEPES buffer), with $C_{Cu^{2+}} = C_{Hcb\text{-}te1pa} = 0.8$ mM. Additionally, complex formation was also studied at pH 3.0 [0.2 M (K,H)Cl] under pseudo-first-order conditions by following the increasing charge transfer band at 310 nm at $C_{Cu^{2+}} = 10 \times C_{Hcb\text{-}te1pa} = 2$ mM. The acid-assisted dissociation of the copper(II) complex of H**cb-te1pa** was studied under pseudo-first-order conditions in 5 M HCl or 5 M $HClO_4$ aqueous solutions containing the complex at 1.0×10^{-3} M. The solutions of complex and concentrated acid, as well as the spectrophotometer cells, were previously equilibrated at the desired temperature before automatic in-cell absorbance measurements. Concentrated acid was added to sample solutions containing preformed complex without control of ionic strength, and the reaction was followed by the decreasing intensity of the complex's d−d transition band at temperatures of 20, 25, 37, 60, and 90 °C in HCl and at 25 °C in $HClO_4$.

Electrochemical Studies. Cyclic voltammograms were measured using Autolab equipment at rt. All measurements were made using a three-electrode system: a glassy carbon electrode as the working electrode, a platinum wire as the counter-electrode, and a saturated calomel reference electrode. All electrochemical experiments were performed in ca. 1 mM aqueous solutions of preformed complex under a N_2 atmosphere containing 0.1 M $NaClO_4$ as the supporting electrolyte. From the initial potential of the analysis (0 V), the voltage was ramped to −1.3 V, then to 0.2 V, and back to 0 V at a scan rate of 100 mV/s. All potentials are expressed relative to the saturated calomel electrode (SCE) except where otherwise noted.

X-ray Diffraction Studies. X-ray diffraction data were collected with a X-Calibur-2 CCD 4-circle diffractometer (Oxford Diffraction), including a four circle goniometer (KM4) and a two-dimensional CCD detector (SAPPHIRE 2). Three-dimensional X-ray diffraction data were collected on an X-Calibur-2 CCD 4-circle diffractometer (Oxford Diffraction). Data reduction, including interframe scaling, Lorentzian, polarization, empirical absorption, and detector sensitivity corrections, were carried out using programs that are part of CrysAlis software[64] (Oxford Diffraction). Complex scattering factors were taken from the program SHELX97[65] running under the WinGX program system.[66] The structure was solved by direct methods with SIR-97[67] and refined by full-matrix least-squares on F^2. All hydrogen atoms were included in calculated positions and refined in riding mode. Crystal data and details of the data collection and refinement are summarized in Table 6. CCDC 988216 contains the supplementary crystallographic data for this article. These data can be obtained free of charge from the Cambridge Crystallographic Data Centre via www.ccdc.cam.ac.uk/data_request/cif.

Computational Details. All calculations presented in this work were performed employing the Gaussian09 package (revision A.01).[68] Full geometry optimizations of the $[Cu(\mathbf{cb\text{-}te1pa})]^+$ complex were performed in aqueous solution employing DFT within the hybrid meta-GGA approximation with the TPSSh exchange-correlation functional.[69] Input geometries were generated from crystallographic data. In these calculations, we used the standard Ahlrich's valence triple-ξ basis set with polarization functions (TZVP).[70] No symmetry constraints were imposed during the optimizations. In the case of copper complexes, calculations were performed using an unrestricted model; therefore, spin contamination[71] was assessed by a comparison of the expected difference between $S(S + 1)$ for the assigned spin state [$S(S + 1) = 0.75$ for the mononuclear copper(II) complexes investigated here] and the actual value of $\langle S^2 \rangle$.[72] The results obtained indicate that spin contamination is negligible [$\langle S^2 \rangle - S(S + 1) < 0.0020$]. The stationary points found on the potential energy surfaces as a result of geometry optimizations were tested to represent energy minima rather than saddle points via frequency analysis. The default values for the integration grid (75 radial shells and 302 angular points) and the SCF energy convergence criteria (10^{-8}) were used in all calculations. Solvent effects were included by using the polarizable continuum model (PCM), in which the solute cavity is built as an envelope of spheres centered on atoms or atomic groups with appropriate radii. In particular, the integral equation formalism (IEFPCM) variant, as implemented in Gaussian09, was used.[73]

dx.doi.org/10.1021/ic500491c | Inorg. Chem. 2014, 53, 5269−5279

Table 6. Crystal Data and Refinement Details for H_3cb-te1pa $(ClO_4)_2$

formula	$C_{19}H_{33}Cl_2N_5O_{10}$
MW	562.40
crystal group	monoclinic
space group	*Cc*
T (K)	170(2)
a (Å)	11.1484(9)
b (Å)	14.8319(12)
c (Å)	14.8211(11)
α (deg)	90
β (deg)	98.561(8)
γ (deg)	90
V (Å^3)	2423.4(3)
F(000)	1184
Z	4
λ (Å) (Mo K_α)	0.710 73
D_{calc} (g cm^{-3})	1.541
μ (mm^{-1})	0.333
θ range (deg)	3.39 to 26.37
R_{int}	0.0508
reflns measd	9238
unique reflns	4053
reflns obsd	2501
GOF on F^2	0.901
R_1[a]	0.0911
wR_2 (all data)[b]	0.1261
largest differences peak and hole (e Å^{-3})	0.655 and −0.610

[a] $R_1 = \Sigma||F_o| - |F_c||/\Sigma|F_o|$. [b] $wR_2 = \{\Sigma(F_o^2 - F_c^2)^2/\Sigma w(F_o^4)\}^{1/2}$.

■ ASSOCIATED CONTENT

Supporting Information

Selected bond lengths and angles and view of the [Cu(**cb-te1pa**)]$(ClO_4)_2$ X-ray structure; ^{1}H NMR titration of H**cb-te1pa** in D_2O; speciation diagrams of Cu^{2+} and Zn^{2+} H**cb-te1pa** complexes; UV and vis-NIR spectra of the copper(II) complex of H**cb-te1pa**; ^{1}H and ^{13}C NMR spectra of [Zn(**cb-te1pa**)]$^+$ at different temperatures; time course of the copper(II) complexation by H**cb-te1pa**; Arrhenius plot for the acid-assisted dissociation of the copper(II) complex of H**cb-te1pa**; optimized Cartesian coordinates obtained with DFT calculations for [Cu(**cb-te1pa**)]$^+$; compound analyses; and X-ray crystal structures in CIF format. This material is available free of charge via the Internet at http://pubs.acs.org.

■ AUTHOR INFORMATION

Corresponding Authors

*(R.D.) E-mail: delgado@itqb.unl.pt.

*(R.T.) E-mail: Raphael.Tripier@univ-brest.fr.

Notes

The authors declare no competing financial interest.

■ ACKNOWLEDGMENTS

R.T. acknowledges the Ministère de l'Enseignement Supérieur et de la Recherche, the Centre National de la Recherche Scientifique, the ANR program αRIT/βPET, and especially the financial support from the Région Bretagne and Europa, France. R.T. also thanks the "Service Commun" of the NMR facilities at the University of Brest. C.P.-I. acknowledges Centro de Supercomputación de Galicia (CESGA) for providing the computer facilities. L.M.P.L. thanks the Fundação para a Ciência e a Tecnologia (FCT) for a postdoctoral fellowship (SFRH/BPD/73361/2010). The Bruker Avance II+ 400 NMR spectrometer used in this work is part of the National NMR Facility, for which we are also thankful for the support from the FCT (RECI/BBB-BQB/0230/2012).

■ REFERENCES

(1) Wadas, T. J.; Wong, E. H.; Weisman, G. R.; Anderson, C. J. *Curr. Pharm. Des.* **2007**, *13*, 3−16.

(2) Wadas, T. J.; Wong, E. H.; Weisman, G. R.; Anderson, C. J. *Chem. Rev.* **2010**, *110*, 2858−2902.

(3) Cutler, C.; Hennkens, H.; Sisay, N.; Huclier-Markai, S.; Jurisson, S. *Chem. Rev.* **2013**, *113*, 858−883.

(4) Shokeen, M.; Anderson, C. J. *Acc. Chem. Res.* **2009**, *42*, 832−841.

(5) Anderson, C. J.; Wadas, T. J.; Wong, E. H.; Weisman, G. R. *Q. J. Nucl. Med. Mol. Imaging* **2008**, *52*, 185−192.

(6) Mewis, R. E.; Archibald, S. J. *Coord. Chem. Rev.* **2010**, *254*, 1686−1712.

(7) Silversides, J. D.; Smith, R.; Archibald, S. J. *Dalton Trans.* **2011**, *40*, 6289−6297.

(8) Ramogida, C. F.; Orvig, C. *Chem. Commun.* **2013**, *49*, 4720−4739.

(9) Liu, S. *Adv. Drug Delivery Rev.* **2008**, *60*, 1347−1370.

(10) Odendaal, Y.; Fiamengo, A. L.; Ferdani, R.; Wadas, T. J.; Hill, D. C.; Peng, Y.; Heroux, K. J.; Golen, J. A.; Rheingold, A. L.; Anderson, C. J.; Weisman, G. R.; Wong, E. H. *Inorg. Chem.* **2011**, *50*, 3078−3086.

(11) Pandya, D. N.; Dale, A. V.; Kim, J. Y.; Lee, H.; Su, H. Y.; Il An, G.; Yoo, J. *Bioconjugate Chem.* **2012**, *23*, 330−335.

(12) Esteves, C. V.; Lamosa, P.; Delgado, R.; Costa, J.; Désogère, P.; Rousselin, Y.; Goze, C.; Denat, F. *Inorg. Chem.* **2013**, *52*, 5138−5153.

(13) Boswell, C. A.; Sun, X.; Niu, W.; Weisman, G. R.; Wong, E. H.; Rheingold, A. L.; Anderson, C. J. *J. Med. Chem.* **2004**, *47*, 1465−1474.

(14) Lewis, E. A.; Boyle, R. W.; Archibald, S. J. *Chem. Commun.* **2004**, 2212−2213.

(15) Sprague, J. E.; Peng, Y.; Fiamengo, A. L.; Woodin, K. S.; Southwick, E. A.; Weisman, G. R.; Wong, E. H.; Golen, J. A.; Rheingold, A. L.; Anderson, C. J. *J. Med. Chem.* **2007**, *50*, 2527−2535.

(16) Boswell, C. A.; Regino, C. A. S.; Baidoo, K. E.; Wong, K. J.; Bumb, A.; Xu, H.; Milenic, D. E.; Kelley, J. A.; Lai, C. C.; Brechbiel, M. W. *Bioconjugate Chem.* **2008**, *19*, 1476−1484.

(17) Boros, E.; Rybak-Akimova, E.; Holland, J. P.; Rietz, T.; Rotile, N.; Blasi, F.; Day, H.; Latifi, R.; Caravan, P. *Mol. Pharmaceutics* **2014**, *11*, 617−629.

(18) Stigers, D. J.; Ferdani, R.; Weisman, G. R.; Wong, E: H.; Anderson, C. J.; Golen, J. A.; Moored, C.; Rheingold, A. L. *Dalton Trans.* **2010**, *39*, 1699−1701.

(19) Ferdani, R.; Stigers, D. J.; Fiamengo, A. L.; Wei, L.; Li, B. T. Y.; Golen, J. A.; Rheingold, A. L.; Weisman, G. R.; Wong, E. H.; Anderson, C. J. *Dalton Trans.* **2012**, *41*, 1938−1950.

(20) (a) Ferreiros-Martinez, R.; Platas-Iglesias, C.; de Blas, A.; Esteban-Gomez, D.; Rodriguez-Blas, T. *Eur. J. Inorg. Chem.* **2010**, 2495−2503. (b) Ferreiros-Martinez, R.; Esteban-Gomez, D.; Toth, E.; de Blas, A.; Platas-Iglesias, C.; Rodriguez-Blas, T. *Inorg. Chem.* **2011**, *50*, 3772−3784. (c) Ferreiros-Martinez, R.; Esteban-Gomez, D.; de Blas, A.; Platas-Iglesias, C.; Rodriguez-Blas, T. *Inorg. Chem.* **2009**, *48*, 11821−11831.

(21) Ferreiros-Martinez, R.; Esteban-Gomez, D.; Platas-Iglesias, C.; de Blas, A.; Rodriguez-Blas, T. *Dalton Trans.* **2008**, 5754−5758.

(22) Boros, E.; Ferreira, C.; Cawthray, J.; Price, E.; Patrick, B.; Wester, D.; Adam, M.; Orvig, C. *J. Am. Chem. Soc.* **2010**, *132*, 15726−15733.

(23) Boros, E.; Cawthray, J. F.; Ferreira, C. L.; Patrick, B. O.; Adam, M. J.; Orvig, C. *Inorg. Chem.* **2012**, *51*, 6279−6284.

(24) Lima, L. M. P.; Esteban-Gómez, D.; Delgado, R.; Platas-Iglesias, C.; Tripier, R. *Inorg. Chem.* **2012**, *51*, 6916−6927.

(25) Frindel, M.; Camus, N.; Rauscher, A.; Bourgeois, M.; Alliot, C.; Barré, L.; Gestin, J.-F.; Tripier, R.; Faivre-Chauvet, A. *Nucl. Med. Biol.* [Online early access.] DOI: 10.1016/j.nucmedbio.2013.12.009. Published Online: Dec 18, **2013**.

(26) Roger, M.; Lima, L. M. P.; Frindel, M.; Platas-Iglesias, C.; Gestin, J.-F.; Delgado, R.; Patinec, V.; Tripier, R. *Inorg. Chem.* **2013**, *52*, 5246−5259.
(27) Wong, E. H.; Weisman, G. R.; Hill, D. C.; Reed, D. P.; Rogers, M. E.; Condon, J. S.; Fagan, M. A.; Calabrese, J. C.; Lam, K.-C.; Guzei, I. A.; Rheingold, A. L. *J. Am. Chem. Soc.* **2000**, *122*, 10561−10572.
(28) Mato-Iglesias, M.; Roca-Sabio, A.; Pálinkás, Z.; Esteban-Gómez, D.; Platas-Iglesias, C.; Tóth, E.; de Blas, A.; Rodríguez-Blas, T. *Inorg. Chem.* **2008**, *47*, 7840−7851.
(29) Weisman, G. R.; Rogers, M. E.; Wong, E. H.; Jasinski, J. P.; Paight, E. S. *J. Am. Chem. Soc.* **1990**, *112*, 8604−8605.
(30) Bencini, A.; Bianchi, A.; Bazzicalupi, C.; Ciampolini, M.; Fusi, V.; Micheloni, M.; Nardi, N.; Paoli, P.; Valtancoli, B. *Supramol. Chem.* **1994**, *3*, 141−146.
(31) Hubin, T. J.; McCormick, J. M.; Collinson, S. R.; Buchalova, M.; Perkins, C. M.; Alcock, N. W.; Kahol, P. K.; Raghunathan, A.; Busch, D. H. *J. Am. Chem. Soc.* **2000**, *122*, 2512−2522.
(32) Hubin, T. J.; Alcock, N. W.; Clase, H. J.; Busch, D. H. *Supramol. Chem.* **2001**, *13*, 261−276.
(33) Bernier, N.; Costa, J.; Delgado, R.; Félix, V.; Royale, G.; Tripier, R. *Dalton Trans.* **2011**, *40*, 4514−4526.
(34) Sun, X.; Wuest, M.; Weisman, G. R.; Wong, E. H.; Reed, D. P.; Boswell, C. A.; Motekaitis, R.; Martell, A. E.; Welch, M. J.; Anderson, C. J. *J. Med. Chem.* **2002**, *45*, 469−477.
(35) Delgado, R.; Sun, Y.; Motekaitis, R. J.; Martell, A. E. *Inorg. Chem.* **1993**, *32*, 3320−3326.
(36) Addison, A. W.; Nageswara-Rao, T.; Reedijk, J.; van Rijn, J.; Verschoor, G. C. *J. Chem. Soc., Dalton Trans.* **1984**, 1349−1356.
(37) Liang, X.; Sadler, P. J. *Chem. Soc. Rev.* **2004**, *33*, 246−266.
(38) Dale, J. *Acta Chem. Scand.* **1973**, *27*, 1115−1129.
(39) Platas-Iglesias, C.; Mato-Iglesias, M.; Djanashvili, K.; Muller, R. N.; Elst, L. V.; Peters, J. A.; de Blas, A.; Rodríguez-Blas, T. *Chem.—Eur. J.* **2004**, *10*, 3579−3590.
(40) Lever, A. B. P. *Inorganic Electronic Spectroscopy*, 2nd ed., Elsevier: New York, 1984; pp 554−572.
(41) Hathaway, B. J. *Coord. Chem. Rev.* **1983**, *52*, 87−169.
(42) Simulations of EPR spectra were performed with the SpinCount software, created by Prof. M. P. Hendrich at Carnegie Mellon University. SpinCount is available at http://www.chem.cmu.edu/groups/hendrich/.
(43) Hathaway, B. J.; Tomlinson, A. A. G. *Coord. Chem. Rev.* **1970**, *5*, 1−43.
(44) Hathaway, B. J.; Billing, D. E. *Coord. Chem. Rev.* **1970**, *5*, 143−207.
(45) Bertini, I.; Gatteschi, D.; Scozzafava, A. *Inorg. Chem.* **1977**, *16*, 1973−1976.
(46) Halcrow, M. A. *Dalton Trans.* **2003**, 4375−4384.
(47) Garribba, E.; Micera, G. *J. Chem. Educ.* **2006**, *83*, 1229−1232.
(48) Billing, D. E.; Hathaway, B. J. *J. Chem. Soc. A* **1969**, 1192−1197.
(49) Harris, R. K. *Nuclear Magnetic Resonance Spectroscopy: A Physicochemical View*; Pitman: London, 1983.
(50) (a) Liang, X.; Weishäupl, M.; Parkinson, J. A.; Parsons, S.; McGregor, P. A.; Sadler, P. J. *Chem.—Eur. J.* **2003**, *9*, 4709−4717. (b) Buckingham, D. A.; Clark, C. R.; Rogers, A. J. *J. Am. Chem. Soc.* **1997**, *119*, 4050−4058. (c) Rodríguez-Rodríguez, A.; Esteban-Gómez, D.; de Blas, A.; Rodríguez-Blas, T.; Fekete, M.; Botta, M.; Tripier, R.; Platas-Iglesias, C. *Inorg. Chem.* **2012**, *51*, 2509−2521.
(51) Hubin, T. J.; McCormick, J. M.; Collinson, S. R.; Alcock, N. W.; Busch, D. H. *Chem. Commun.* **1998**, 1675−1676.
(52) Woodin, K. S.; Heroux, K. J.; Boswell, C. A.; Wong, E. H.; Weisman, G. R.; Niu, W.; Tomellini, S. A.; Anderson, C. J.; Zakharov, L. N.; Rheingold, A. L. *Eur. J. Inorg. Chem.* **2005**, 4829−4833.
(53) Heroux, K. J.; Woodin, K. S.; Tranchemontagne, D. J.; Widger, P. C. B.; Southwick, E.; Wong, E. H.; Weisman, G. R.; Tomellini, S. A.; Wadas, T. J.; Anderson, C. J.; Kassel, S.; Golen, J. A.; Rheingold, A. L. *Dalton Trans.* **2007**, 2150−2162.
(54) Chen, L.-H.; Chung, C.-S. *Inorg. Chem.* **1988**, *27*, 1880−1883.
(55) Kotek, J.; Lubal, P.; Hermann, P.; Císařová, I.; Lukeš, I.; Godula, T.; Svobodová, I.; Táborský, P.; Havel, J. *Chem.—Eur. J.* **2003**, *9*, 233−248.
(56) Basallote, M. G.; Castillo, C. E.; Máñez, M. A.; Lubal, P.; Martínez, M.; Rodríguez, C.; Vaněk, J. *Inorg. Chem. Commun.* **2010**, *13*, 1272−1274.
(57) Wolsey, W. C. *J. Chem. Educ.* **1973**, *50*, A335−A336.
(58) Rossotti, F. J.; Rossotti, H. J. *J. Chem. Educ.* **1965**, *42*, 375−378.
(59) Schwarzenbach, G.; Flaschka, W. *Complexometric Titrations*; Methuen & Co: London, 1969.
(60) Calibration software from the maker of Hyperquad is available for free at http://www.hyperquad.co.uk/.
(61) Gans, P.; Sabatini, A.; Vacca, A. *Talanta* **1996**, *43*, 1739−1753.
(62) Alderighi, L.; Gans, P.; Ienco, A.; Peters, D.; Sabatini, A.; Vacca, A. *Coord. Chem. Rev.* **1999**, *184*, 311−318.
(63) Delgado, R.; Fraústo da Silva, J. J. R.; Amorim, M. T. S.; Cabral, M. F.; Chaves, S.; Costa, J. *Anal. Chim. Acta* **1991**, *245*, 271−282.
(64) (a) *CrysAlis CCD*, version 1.171.33.52; Oxford Diffraction Ltd.: Oxfordshire, UK, 2009. (b) *CrysAlis RED*, version 1.171.33.52; Oxford Diffraction Ltd.: Oxfordshire, UK, **2009**.
(65) Sheldrick, G. M. *Acta Crystallogr.* **2008**, *A64*, 112−122.
(66) Farrugia, L. J. *J. Appl. Crystallogr.* **1999**, *32*, 837−838.
(67) Altomare, A.; Burla, M. C.; Camalli, M.; Cascarano, G. L.; Giacovazzo, C.; Guagliardi, A.; Moliterni, A. G. G.; Polidori, G.; Spagna, R. *J. Appl. Crystallogr.* **1999**, *32*, 115−119.
(68) Frisch, M. J.; Trucks, G. W.; Schlegel, H. B.; Scuseria, G. E.; Robb, M. A.; Cheeseman, J. R.; Scalmani, G.; Barone, V.; Mennucci, B.; Petersson, G. A.; Nakatsuji, H.; Caricato, M.; Li, X.; Hratchian, H. P.; Izmaylov, A. F.; Bloino, J.; Zheng, G.; Sonnenberg, J. L.; Hada, M.; Ehara, M.; Toyota, K.; Fukuda, R.; Hasegawa, J.; Ishida, M.; Nakajima, T.; Honda, Y.; Kitao, O.; Nakai, H.; Vreven, T.; Montgomery, Jr., J. A.; Peralta, J. E.; Ogliaro, F.; Bearpark, M.; Heyd, J. J.; Brothers, E.; Kudin, K. N.; Staroverov, V. N.; Kobayashi, R.; Normand, J.; Raghavachari, K.; Rendell, A.; Burant, J. C.; Iyengar, S. S.; Tomasi, J.; Cossi, M.; Rega, N.; Millam, N. J.; Klene, M.; Knox, J. E.; Cross, J. B.; Bakken, V.; Adamo, C.; Jaramillo, J.; Gomperts, R.; Stratmann, R. E.; Yazyev, O.; Austin, A. J.; Cammi, R.; Pomelli, C.; Ochterski, J. W.; Martin, R. L.; Morokuma, K.; Zakrzewski, V. G.; Voth, G. A.; Salvador, P.; Dannenberg, J. J.; Dapprich, S.; Daniels, A. D.; Farkas, Ö.; Foresman, J. B.; Ortiz, J. V.; Cioslowski, J.; Fox, D. J. *Gaussian09*, Revision A.01; Gaussian, Inc.: Wallingford, CT, 2009.
(69) Tao, J. M.; Perdew, J. P.; Staroverov, V. N.; Scuseria, G. E. *Phys. Rev. Lett.* **2003**, *91*, 146401.
(70) Schaefer, A.; Huber, C.; Ahlrichs, R. *J. Chem. Phys.* **1994**, *100*, 5829−5835.
(71) Stanton, J. F.; Gauss, J. *Adv. Chem. Phys.* **2003**, *125*, 101−146.
(72) Montoya, A.; Truong, T. N.; Sarofim, A. F. *J. Phys. Chem. A* **2000**, *124*, 6108−6110.
(73) Tomasi, J.; Mennucci, B.; Cammi, R. *Chem. Rev.* **2005**, *105*, 2999−3093.

NOTE ADDED AFTER ASAP PUBLICATION

This paper was published on the Web on April 23, 2014, with errors in Table 2. The corrected version was reposted on April 25, 2014.